

Rapid Generation of Composition Profiles for Reactive and Extractive Cascades

James Chin and Jae W. Lee

Dept. of Chemical Engineering, The City College of the City University of New York, New York, NY 10031

DOI 10.1002/aic.10343

Published online in Wiley InterScience (www.interscience.wiley.com).

A quick method for estimating composition profiles for reactive and extractive cascades in a double-feed column without stage calculations is presented. This profile estimation is based on the feasibility and pinch point analyses. The trajectories of pinch points are determined with material balance equations and phase and reaction equilibrium data. From these pinch point trajectories, the ranges of feasible external reflux ratios and required entrainer flow rates are calculated for a given reaction extent and product purity. Then, for given external reflux ratios, heat balance constraints are imposed to determine the positions of pinch points. Finally, using the internal reflux ratios of these pinch points, manifolds of possible composition profiles are generated. Composition profiles of a reactive/extractive cascade can lie in the section of the reaction equilibrium surface where the internal reflux ratio of a saddle pinch is between the upper and lower bounds of the internal reflux ratio. © 2005 American Institute of Chemical Engineers AIChE J, 51: 922–930, 2005

Keywords: Composition profiles, reactive and extractive cascade, pinch points

Introduction

Extractive distillation has been used for separating azeotropic mixtures or other mixtures with low relative volatilities. It can also be combined with reaction to circumvent azeotropic compositions. A representative example is Eastman's system for producing methyl acetate by reactive distillation^{1–2}. In this reactive extractive distillation, one minimum boiling azeotrope between methyl acetate (MA) and methanol (MT) is broken through the complete consumption of MT in the reaction, while the other azeotrope between MA and water (W) is circumvented by extractive distillation with acetic acid (AC).

Extractive distillation columns are feasible if an extractive agent and a desired top product are dominantly present at the extractive (or upper) feed stage. Thus, the composition profile around the extractive feed stage approaches or lies on the binary edge between those two components in composition space^{3–6}. This feasibility consideration is also applicable to

reactive extractive distillation in a double-feed column⁷. For example, the composition profile of the MA reactive distillation column approaches the binary edge of extractive agent (and reactant) AC and product MA while moving up the column from the lower feed stage to the upper feed stage. If a binary mixture of AC and MA exists at the upper feed stage, then the nonreactive rectifying section above that stage can separate pure MA from the binary mixture since no minimum-boiling azeotrope exists between AC and MA.

Using the above simple feasibility information, this article will address how to determine feasible composition profiles for double-feed distillation columns, based on the concept of the upper and lower bounds of the internal reflux ratio⁷ and the stability analysis of pinch points^{8–10}.

This work will review the first key concept of the upper and lower reflux ratios. The upper and lower bounds of the internal reflux ratio are determined from the phase equilibrium behavior of the system, the feed and product specifications, and an application of material balance constraints. This application of material balance constraints will determine the set of all possible pinch points in the middle section of a double-feed column. An eigenvalue analysis will be used to determine

Correspondence concerning this article should be addressed to J. W. Lee at J.lee@ccny.cuny.edu.

Material and energy balance envelope

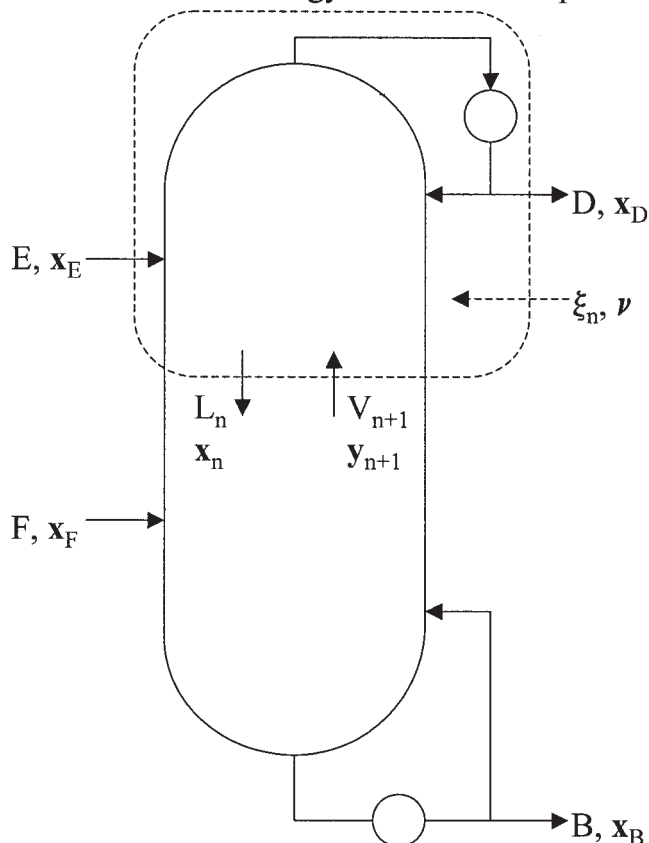


Figure 1. Double feed extractive/reactive distillation column.

$\xi_n = 0$ for a nonreactive case and $\xi_n \neq 0$ for a reactive case.

which possible pinch points are stable or unstable nodes and which are saddle points.

Then, for a given external reflux ratio (that is, for a given heat balance), it will be shown that the internal reflux ratio of the saddle pinch point lies between the upper and lower bounds of the internal reflux ratio of every stage in the middle section composition profile. Thus, the manifold of all possible composition profiles for the middle section can be drawn for any desired external reflux ratio by calculating the upper and lower bounds at every point in composition space. Rigorous stage calculations are used to verify this method. Two real systems will be intensively considered in this article: the nonreactive acetone (AT)—MT—W system, and the reactive MA production system.

Upper and Lower Reflux Ratios for a Non-reactive System

As shown in Figure 1, a material balance envelope is drawn from the top of the column to an arbitrary stage (n) in the middle section of the column. Here, we consider nonreactive extractive distillation, so ξ_n in Figure 1 is equal to zero. Column parameters are specified: namely, the ratio of the extractive feed and the distillate molar flow rates (E/D), the distillate composition (x_D), and the extractive feed composition (x_E). Then, an arbitrary composition is selected and is assumed

to be the liquid-phase composition on the arbitrary stage (x_n). It is then of interest to determine whether or not a column profile passing through this arbitrary composition can reach the binary edge of an extractive agent and a top product.

This determination begins with the assumption that this arbitrary stage is pinched. Therefore, the vapor stream (y_{n+1}) entering the material balance envelope is identical to the vapor stream (y_n) that is in phase equilibrium with the liquid stream (x_n) leaving the material balance envelope. With these liquid and vapor compositions (y_n and x_n), and the compositions of the distillate (x_D), and the extractive feed (x_E), material balance lines are drawn in composition space according to the following material balance equations

$$L_n x_n + D x_D = V_n y_n + E x_E = (L_n + D) x^* = (V_n + E) x^* \quad (1)$$

$$L_n x_n + D x_D = (L_n + D) x^* \quad \frac{L_n}{D} = \frac{\overline{x^* x_D}}{\overline{x^* x_n}} \quad (2)$$

$$V_n y_n + E x_E = (V_n + E) x^* \quad \frac{V_n}{E} = \frac{\overline{x^* x_E}}{\overline{x^* y_n}} \quad (3)$$

where x^* is the point of intersection of the material balance lines, L_n is the liquid molar flow rate leaving stage n , V_n is the vapor molar flow rate leaving stage n , D is the molar flow rate of the distillate, and E is the molar flow rate of the extractive feed. An overbar refers to the length of a line segment connecting two points on a composition diagram. For example, $\overline{x^* x_D}$, indicates the length of the line segment connecting x^* and x_D .

Through the use of the lever rule shown in Eqs 2 and 3, the ratios of the lengths of line segments are related to the ratios of flow rates in and out of the material balance envelope, thus, providing for two different means of calculating the internal reflux ratio on this stage. The ratio of the lengths of the line segments labeled L_n and D in Figure 2 is taken as the internal reflux ratio because the internal reflux ratio for a particular stage n is defined as L_n/D . The ratio of the lengths of the line

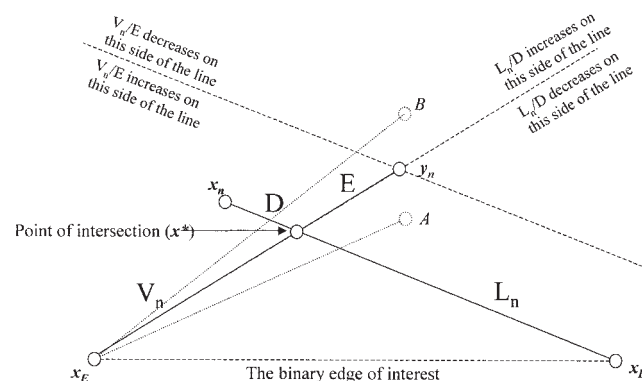


Figure 2. Calculation of the upper and lower bounds of the IRR in the acetone-methanol-water system.

A and B denote possible y_{n+1} .

segments labeled V_n and E are related to the internal reflux ratio by manipulating the total molar material balance equation in the following manner

$$L_n + D = V_n + E \quad (4)$$

$$\frac{L_n}{D} + 1 = \frac{V_n}{D} + \frac{E}{D} \quad (5)$$

$$\frac{L_n}{D} = \frac{V_n}{E} \frac{E}{D} + \frac{E}{D} - 1 \quad (6)$$

If the stage under consideration were actually pinched and E is equal to D ($E/D = 1$), then the two calculated values of the reflux ratio (L_n/D and V_n/E) would be equal in Eq. 6. However, since a liquid-phase composition was arbitrarily chosen, the stage is most likely not pinched and the two calculated values for the internal reflux ratio are different. We recall that it is desired to approach a particular boundary of the composition space (the AT-W binary edge in this example), while going up the middle-section between the two-feed stages. Therefore, the composition of the vapor stream entering the material balance envelope (y_{n+1}) must be further away from this binary edge than the composition of the vapor stream leaving stage n (y_n). If this is not the case, then the composition profile will head away from the binary edge while moving up to the upper feed stage. Geometrical considerations then dictate that one of the calculated ratios has to be greater than the other calculated ratio in order for a column composition profile passing through this point (x_n) to reach the binary edge. These two calculated ratios are therefore called the upper and lower bounds of the internal reflux ratio.

Again consider Figure 2. Suppose that y_{n+1} is closer to the desired edge than y_n (at point A); this would represent an infeasible case as the column composition profile would head away from the binary edge while going up the column from stage $n+1$ to stage n . If the true y_{n+1} were used to redraw the material balance lines, then the true internal reflux ratio would be less than L_n/D and greater than V_n/E . Now suppose that y_{n+1} was further away from the desired edge than y_n (at point B in Figure 2); this would represent a feasible case as the column composition profile would head toward the binary edge, while going up the column from stage $n+1$ to stage n . In this case, if the true y_{n+1} were used to redraw the material balance lines, then the true internal reflux ratio would be greater than L_n/D and less than V_n/E . Hence, L_n/D is referred to as the lower bound of the internal reflux ratio and V_n/E is used to calculate the upper bound of the internal reflux ratio by the use of Eq. 6 shown earlier.

A feasible composition profile can pass through a liquid-phase composition (x_n) when the upper reflux ratio is greater than the lower reflux ratio at that x_n . Under arbitrary E/D ratios, the upper and lower reflux ratios are the right and left sides, respectively, of Eq. 6. This calculation can be quickly and easily repeated using any phase-equilibrated pair of compositions x_n and y_n in composition space. Thus, it is possible to draw a region in composition space where the upper bound is greater than the lower bound; this is the region where column composition profiles head toward the binary edge.

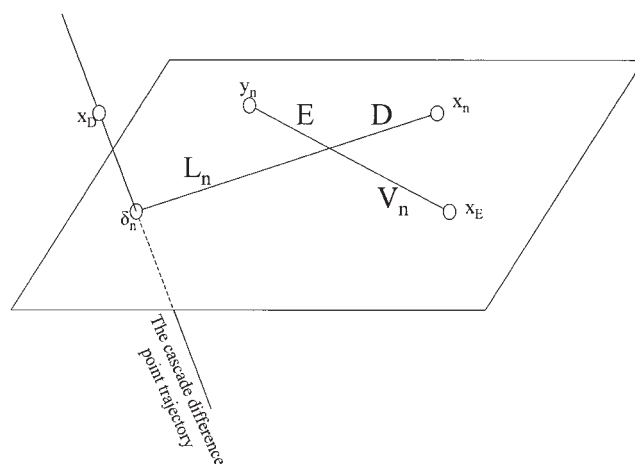


Figure 3. Calculation of the upper and lower bounds of the IRR for the methyl acetate production system.

Upper and Lower Reflux Ratios for a Reactive System

In the AT-MT-W system, drawing these material balance lines is a simple matter as we only require that the two material balance lines intersect in a two-dimensional (2-D) (three-component) composition space as shown in Figure 2. However, in the reactive MA production system, the points used to draw the liquid, vapor, extractive, and distillate compositions do not lie on the same plane in composition space.

Lee (2002)⁷ proposed the following: given a distillate composition and the reaction stoichiometry, a line can be drawn on a composition diagram through the distillate composition and parallel to the reaction stoichiometry vector. This line is called the “cascade difference point trajectory” and combines the distillate and reaction terms of the material balance equations¹¹⁻¹². For any given liquid composition (x_n) on a hypothetical stage in the reactive section of the column, Lee (2002)⁷ shows that there exists a unique point on this trajectory called the “cascade difference point” such that material balance lines can be drawn. Specifically, this is the point where the cascade difference trajectory intersects the plane containing the liquid, vapor, and extractive feed compositions as shown in Figure 3. The lever rule is then applied to the segments of the material balance lines to determine the upper and lower bounds of the reflux ratio with the simple modification that the cascade difference point, δ_n , is used in these calculations instead of the distillate composition x_D .

The upper and lower reflux calculations required only phase equilibrium information, material balance constraints, the extractive feed composition, the desired distillate composition, and the ratio of the extractive and distillate flow rates. In the reactive case, reaction stoichiometry and reaction equilibrium information were also used. From these upper bound and lower bound calculations, the region where the upper bound is greater than the lower bound can be drawn. A column profile must travel through this region in order to reach the binary edge of the extractive feed composition and the desired distillate product composition.

Since possible pinch points exist wherever the upper bound equals the lower bound, this region is bound by the pinch point

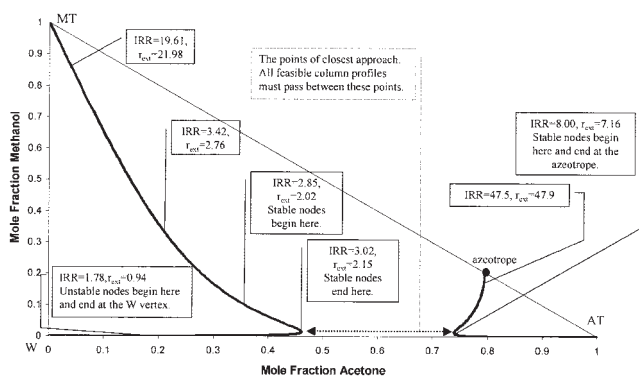


Figure 4. Pinch point trajectories for the acetone-methanol-water system.

Given conditions³ are $x_E = [0.000004 \ 0.000496 \ 0.9995]$ and $x_D = [0.995 \ 0.001 \ 0.004]$ for AT, MT, and W, respectively, $E/D = 1.0955$. All pinch points are saddles unless otherwise marked.

trajectories. If the upper and lower bounds are calculated at points sampled throughout composition space, then this region is easily visible and the boundaries of this region are the pinch point trajectories. In both Figure 4 (for the AT-MT-W system) and Figure 5 (for the MA production system), it can be seen that there are two pinch point trajectories between which the upper bounds are greater than the lower bounds. These figures also show the nature of the pinch points and their internal/external reflux ratios (IRR/ r_{ext}), which will be discussed in the following section.

Determination of Pinch Point Trajectories

In the previous section, it was shown how the pinch point trajectories could be located by sampling points in composition space and selecting those points where the upper and lower bounds of the internal reflux ratio are equal. Although effective in quickly determining the approximate locations of pinch trajectories, this method is slightly time-consuming when trying to locate these trajectories with precision. Thus, this section will show the mathematical determination of the pinch point trajectories by using material balance constraints and equilibrium data.

The pinch point trajectories in the AT-MT-W system can be described by the following N_{comp} molar component material balance equations

$$\frac{V_n}{D} y_{n,i} + \frac{E}{D} x_{E,i} - \frac{L_n}{D} x_{n,i} - x_{D,i} = 0 \quad \text{for } i = 1 \dots N_{comp} \quad (7)$$

where $(V_n/D) = (L_n/D) + 1 - (E/D)$, N_{comp} is the number of components, and $y_{n,i}$ is the vapor phase fraction of component i (a function of the liquid phase composition). In the MA system, there is also a reaction term, $(\xi_n/D) \nu_i$, on the left-hand side of each occurrence of Eq. 7 where ξ_n is the molar extent of reaction on all of the trays in the material balance envelope and ν_i is the reaction stoichiometry coefficient of component i .

The MA production system also has an additional equation that requires any liquid phase composition to be on the reaction

equilibrium surface (because the reaction takes place in the liquid phase)

$$K_{equil} = \frac{x_{n,MA} x_{n,W} \gamma_{n,MA} \gamma_{n,W}}{x_{n,AC} x_{n,MT} \gamma_{n,AC} \gamma_{n,MT}} \quad (8)$$

where $x_{n,i}$ and $\gamma_{n,i}$ are the mole fraction and activity coefficient, respectively, of component i and arbitrary stage n and K_{equil} is the reaction equilibrium constant, which is a function of temperature ($K_{equil} = 0.83983 + 782.98/T$ in Song et al., 1998¹³).

Thus, the AT-MT-W system has seven unknowns ((L_n/D) , x_A , x_{MT} , x_W , y_A , y_{MT} , y_W) and six equations (the three material balance equations and the three phase equilibrium equations). The MA production system has ten unknowns ((L_n/D) , (ξ_n/D) , x_{AC} , x_{MT} , x_{MA} , x_W , y_{AC} , y_{MT} , y_{MA} , y_W) and nine equations (the four material balance equations, the four-phase equilibrium equations, and the reaction equilibrium equation). In either case, the pinch trajectory has one degree of freedom. Because the pinch trajectories are dependent on phase equilibrium (which can be severely nonlinear), the trajectories are double-valued at some values of the internal reflux ratio; they cannot be *a priori* relied upon to be single-valued anywhere.

Seyde and Hlavack (1989)¹⁴ and Seider et al. (1991)¹⁵ described what they refer to as the continuation method for calculating trajectories of functions that are not always single valued with respect to a particular continuation parameter. Knapp and Doherty (1994)⁴ performed a bifurcation analysis of such nonlinear systems. The continuation method is applied here in the following manner illustrated in Figure 6: if the coordinates of two closely-spaced points on that trajectory are known ($k-1$ and k), then the coordinates of a third point on the pinch trajectory ($k+1$) can be guessed by drawing a line through the two given points and extending that line some arbitrary distance as shown in Figure 6; where the line ends is an initial guess for the next point on the pinch trajectory ($k+1$).

A linear variation is then drawn through this guessed point

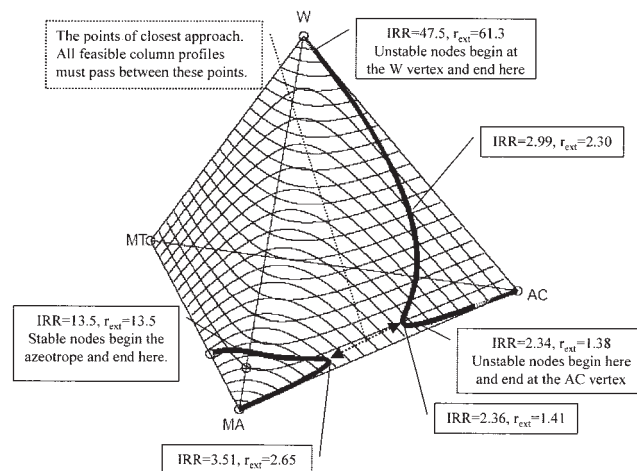


Figure 5. Pinch point trajectories for the methyl acetate production system.

Given conditions⁷ are $x_E = [1 \ 0 \ 0 \ 0]$ and $x_D = [0.001 \ 0.008 \ 0.990 \ 0.001]$ for AC, MT, MA, and W, respectively, $E/D = 1$. All pinch points are saddles unless otherwise marked. Hereafter, open circles are azeotropes and pure component vertices.

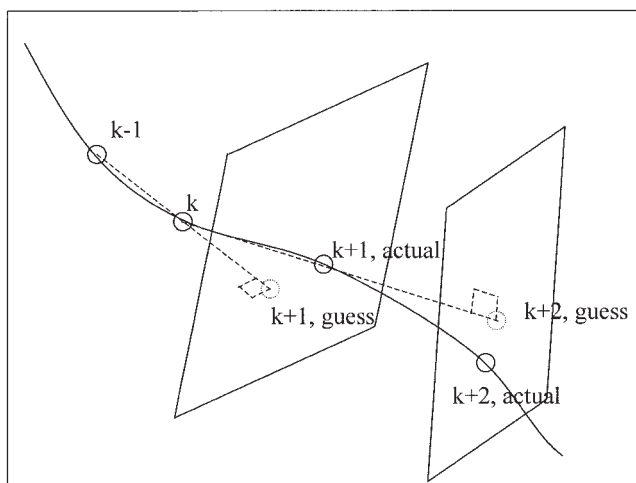


Figure 6. Continuation method for the calculation of pinch trajectories.

and perpendicular to the aforementioned line. The linear variation is represented as a plane in Figure 6, but actually has $N_{param}-1$ dimensions. This linear variation is represented by a single equation and constrains the only degree of freedom held by the pinch trajectory. That equation is

$$0 = \sum_{i=1}^{N_{param}} normal_i(x_i - x_{i,guess}) \quad (9)$$

where N_{param} is the number of continuation method parameters, $normal_i$ is the i -th parameter of the vector pointing from one known point to the other, x_i is the i -th parameter of the coordinates being solved for (the coordinates of the next point on the pinch trajectory), and $x_{i,guess}$ is the i -th parameter of the initial guess for this point. Remember that the parameters are the liquid and vapor mole fractions, the internal reflux ratio, and the extent of reaction (if the system is reactive).

Where the pinch trajectory intersects, this linear variation is the solution to both the equation of the linear variation and the equations that describe the pinch trajectory, and is taken as a third known point on the trajectory ($k+1$). Thus, there is an equation for each unknown, and the set of algebraic equations can be solved by any numerical method found fit for the task (the Newton-Raphson method, for example). The second and third known points (k and $k+1$) are then used to find a fourth point ($k+2$) and repeat the process. Thus, the coordinates of points along the trajectory can be obtained. Because each successive solution is used to calculate the initial guess for the next solution on the trajectory, the method can follow the trajectory regardless of how many twists and turns the trajectory takes as long as the spacing of the two known points being used at each step is sufficiently small (that is, smaller than the radius of curvature of the trajectory at any point on the trajectory).

Once the pinch trajectories are determined by the continuation method, we can also calculate external reflux ratios along the trajectories by applying a heat balance to the envelope shown in Figure 1. The heat balance equation is

$$\frac{V_n}{D} H_n + \frac{E}{D} h_E = \frac{L_n}{D} h_n + h_D - (r_{ext} + 1)(h_D - H_D) \quad (10)$$

where $(V_n/D) = (L_n/D) + 1 - (E/D)$, h_n is the saturated liquid enthalpy of the liquid on the arbitrary stage n , H_n is the saturated vapor enthalpy, also on stage n , h_E is the saturated liquid enthalpy of the upper (extractive) feed stream, and h_D and H_D are the saturated liquid and vapor enthalpies, respectively, of the distillate stream. Then, the external reflux ratio associated with a particular pinch point can be calculated for each point on a pinch trajectory by using Eq. 10 with the internal reflux ratio determined by the continuation method.

In the AT-MT-W system shown in Figure 4, one pinch trajectory travels from the MT vertex to the W vertex. Along this trajectory, the internal and external reflux ratios begin at very large values near the MT vertex and decrease until they each go through a minimum at the point where the saddle pinches become stable nodes. They then increase until they reach the point where the pinches become saddles again. The reflux ratios then decrease again until the pinch points become unstable nodes, and then increase to very large values again as they approach the W vertex. The second trajectory starts at the AT-MT azeotrope, travels toward the W-AT binary edge, and then turns toward the AT vertex. Along this trajectory, the internal and external reflux ratios begin at very high values near the azeotrope, go through minima, and then increase to very large values again as they approach the AT vertex.

In the MA production system shown in Figure 5, one pinch trajectory begins at the W vertex and travels toward the AC vertex. Along this trajectory, the internal and external reflux ratios both start at very high values near the W vertex, go through a minimum, and become very large again as they approach the AC vertex. The other pinch trajectory begins at the MT-MA azeotrope and travels toward the AC-MA binary edge before turning toward the MA vertex. Along this trajectory, the internal and external reflux ratios also begin at very high values, go through minima, and return to very high values again.

The pinch points of any system affect the behavior of column profiles. Hence, the dynamic properties of pinch points are typically of interest. That is, it is usually desired to know whether a pinch point is a stable node, a saddle, or an unstable node. For a particular pinch point, these properties can be determined by calculating the eigenvalues and eigenvectors of the following matrix⁸⁻¹⁰

$$\bar{J} = \left(\frac{\partial f_i}{\partial x_j} \right) \quad i, j = 1 \dots N \text{ comp} \quad (11)$$

where f_i (for the acetone-methanol-water system using the balance envelope described earlier) is defined as $x_{n+1,i} = x_{n,i} = f_i(\bar{x}) = (V_{n+1}/L_n)y_{n+1,i} + (E/L_n)x_{E,i} - (D/L_n)x_{D,i}$, that is, the mole fraction of component i in the liquid phase of stage $n+1$ (which is the same as on stage n , because it is pinched). The MA production system has an additional term, $+(\xi_n/L)v_i$, in the f_i expression.

Julka et al. (1990)⁸ also showed that for an N_{comp} component system, there are $N_{comp}-1$ real, positive eigenvalues. A pinch

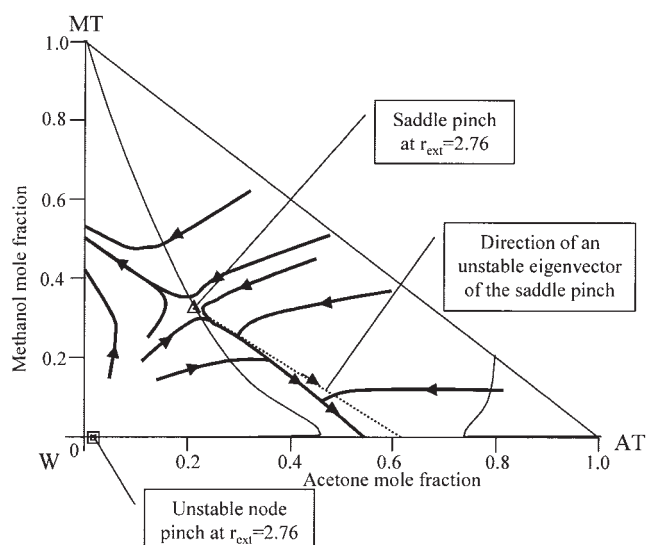


Figure 7. Various tray-by-tray calculated profiles in the acetone-methanol-water system at $r_{\text{ext}} = 2.76$.

point is a stable node if all of its eigenvalues are less than unity. A pinch point is an unstable node if all of its eigenvalues are greater than unity. All other pinch points are saddles and they each have at least one eigenvalue greater than unity and at least one eigenvalue less than unity.

Because we hold the extractive and distillate compositions and their molar flow rates constant, the derivative of f_i is merely a constant times the derivative of y_i , which can be calculated for any analytical representation of the phase equilibrium behavior. In the MA production system, the reaction stoichiometry vector is given and the extent of reaction is prescribed by the reaction equilibrium. Thus, we can also use Eq. 11 for the MA production system to determine eigenvalues and eigenvectors.

Estimation of Operating Parameters and Composition Profiles

General Behavior of Column Profiles

For a given value of the external reflux ratio, it is possible to calculate different middle-section column profiles using various arbitrary starting points throughout composition space as the liquid composition on the tray above the lower feed stage. These rigorously calculated column profiles are plotted in Figure 7 for the AT-MT-W system and Figure 8 for the MA production system.

In the AT-MT-W system of Figure 7, all of the column profiles that begin sufficiently far away from the feasible section of the AT-W edge approach the saddle pinch point before proceeding to either the AT-W or MT-W edges of composition space. Those that go to the AT-W edge are always drawn to the same point on that edge for a given external reflux ratio. Because any middle-section profile must reach the AT-W binary edge to represent a feasible column profile, it should move through the feasible region where the upper reflux bound is greater than the lower reflux bound and then end at the AT-W binary edge. At $r_{\text{ext}} = 2.76$, there are two pinch points present: the saddle pinch at [0.214 0.324 0.462] and an unstable node at

[0.015 0.000 0.985] for AT, MT, and W, respectively. Those profiles that started near the unstable node were first attracted to the saddle before traveling to the AT-W edge.

The tray-by-tray profiles in the MA production system show similar behavior. As shown in Figure 8, all of the feasible composition profiles were attracted to the saddle pinch before traveling to the same spot on the AC-MA binary edge. In the MA production system at $r_{\text{ext}} = 2.3$, there are again two pinch points present: the saddle pinch at [0.536 0.008 0.109 0.347] and an unstable node at [0.874 0.000 0.122 0.005] for AC, MT, MA, and W, respectively.

Brüggemann and Marquardt (2004)¹⁶ discussed a profile estimation, based on the calculation of the eigenvectors of the pinch points of the system and take the direction of the eigenvectors as being the direction of the nonreactive column profiles. Consistent with their estimate, the column profiles in the AT-MT-W system travel away from the saddle pinch along the unstable eigenvector as shown in Figure 7. The saddle pinch for the MA production system shown in Figure 8 possesses three eigenvectors, one stable and two unstable. The two unstable eigenvectors repel the column profiles away from the saddle pinch and one of them moves toward the feasible destination on the AC-MA binary edge.

The Feasible range of column external reflux ratios

It has been noted that extractive distillation processes exhibit both a minimum and a maximum feasible external reflux ratio^{4-5, 16-17}. As shown in the previous section, the feasible composition profiles always proceed toward, and end in, the region where upper reflux bounds are greater than lower reflux bounds. Thus, for the feasible composition profiles to move toward the AT-W or AC-MA edge, they must pass between the two pinch trajectories as shown in Figures 7 and 8. In each of

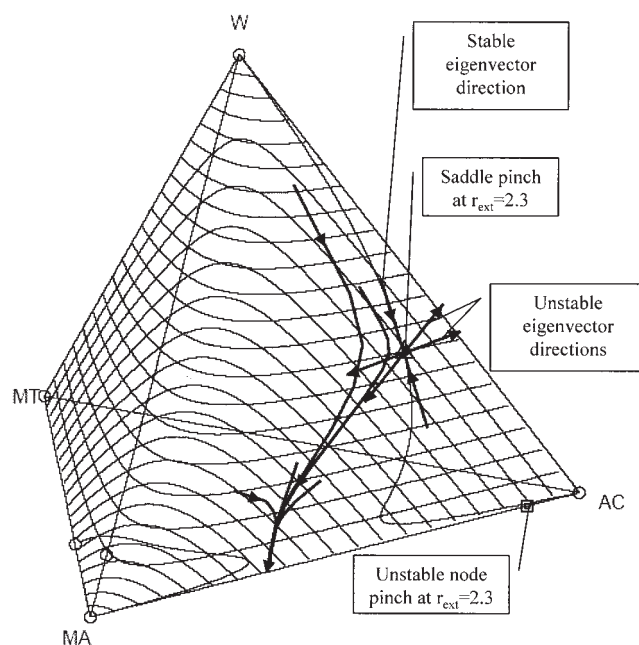


Figure 8. Various tray-by-tray calculated profiles in the methyl acetate production system at $r_{\text{ext}} = 2.30$.

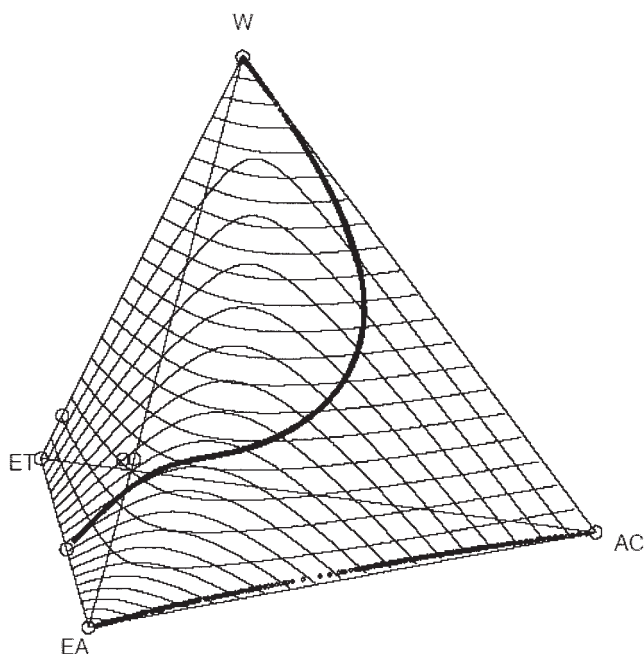


Figure 9. Pinch point trajectories for the ethyl acetate production system with $E/D=1$.

the two systems presented in this article, the two pinch point trajectories have points of closest approach as shown in Figures 4 and 5, that is, points where they come closest to each other. Therefore, all feasible profiles must pass between these two points of closest approach. Then, by using Eq. 10, and the internal reflux ratios (L_n 's) of these pinch points, the range of external reflux ratios that allows feasible operation is determined as 2.2 to 7.2 for the AT-MT-W system and as 1.4 to 2.7 for the MA system for the conditions given in Figures 4 and 5.

The effects of varying E/D

The parameter E/D was fixed when calculating the upper and lower bounds of the internal reflux ratio in the previous sections. However, these upper and lower bounds are dependent on the values of E/D . In some systems, merely combining reaction and separation will not result in the feasible production of pure products from a stoichiometric feed ($E/D = 1$). For example, Figure 9 shows the pinch point trajectories for the ethyl acetate (EA) production system when E/D is equal to 1. There is one trajectory that travels from the W vertex to the ET-EA azeotrope, and a second pinch trajectory that travels from the EA vertex to the AC vertex along the EA-AC edge. Between these two pinch trajectories, the lower bound is greater than the upper bound. It is then clear that pure EA cannot be produced from a stoichiometric feed of ET and AC since the EA-AC binary edge cannot be reached.

However, if E/D is increased to 5 (that is, a 400% AC excess is introduced to act as entrainer), then the pinch point trajectories in Figure 10 result. These trajectories resemble the pinch trajectories shown in Figure 5 for the MA production system; between them, the upper bound is greater than the lower bound and it is possible for feasible column profiles to pass between them to reach the AC-EA edge. By generating pinch trajectories

with different E/D ratios, we can easily determine the feasible ranges of E/D .

Composition profile estimation

The region through which the feasible column profiles travel after turning from the saddle pinch can be determined by first selecting an external reflux ratio and then finding the saddle pinch associated with that external reflux ratio. To determine this region, two conditions will be applied in terms of the concept of the upper and lower reflux ratios and the general behavior of middle section profiles in Figures 7 and 8:

(1) The saddle pinch attracts the feasible composition profiles.

(2) The feasible composition profile must move into the region where the upper bounds of the internal reflux ratio are greater than the lower bounds of the internal reflux ratio and must end in the binary edge connecting the desired top product and upper feed vertices.

To satisfy these two conditions, we can draw the region between the two pinch trajectories where the internal reflux ratio of the saddle pinch lies between the upper and lower bounds of the internal reflux ratio as shown in Figures 11 and 12. Thus, the range of the upper and lower reflux ratios evaluated at this feasible region includes the internal reflux ratio of the saddle pinch.

Figure 11 shows a column composition profile for the middle section of the AT-MT-W system. This profile was generated by a rigorous tray-by-tray algorithm for particular values of x_E , x_D , E/D , and the external reflux ratio. The column profile proceeds from an arbitrarily chosen lower feed stage composition toward a pinch point and then turns to the AT-W binary edge. Notice that while the profile travels from the saddle pinch to the binary edge, it remains inside the feasible region drawn for this system. Figure 12 also shows a rigorously calculated

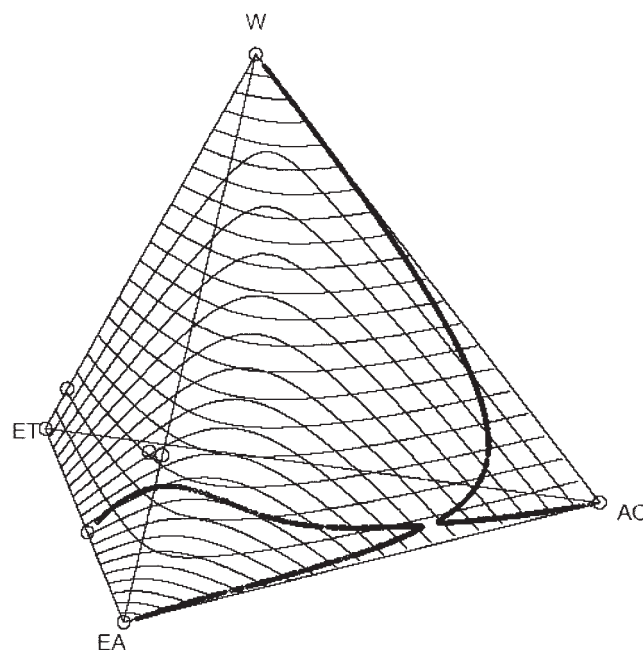


Figure 10. Pinch point trajectories for the ethyl acetate production system with $E/D=5$.

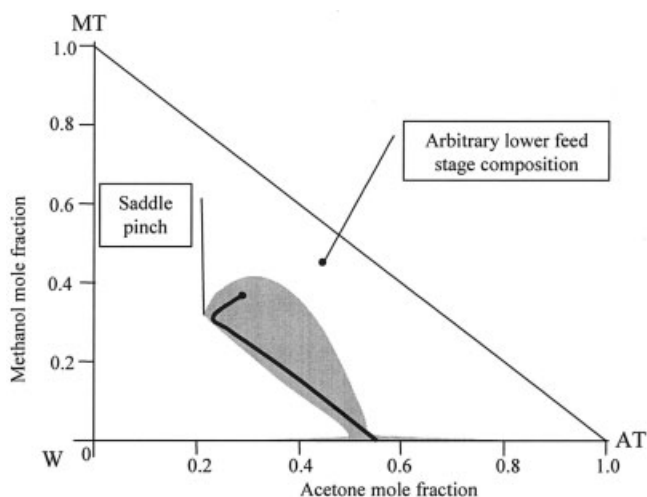


Figure 11. Tray-by-tray-calculated column profile and the feasible region.

$r_{\text{ext}} = 2.76$, IRR of the saddle pinch = 3.42, $x_D = [0.995 \ 0.001 \ 0.004]$, $x_E = [0.000004 \ 0.000496 \ 0.9995]$, $x_F = [0.5 \ 0.5 \ 0]$, $E/D = 1.0955$.

composition profile for the middle section of the MA production system. Again, values of x_E , x_D , E/D , and the external reflux ratio are chosen. This profile also travels from the arbitrarily chosen lower feed stage composition toward the saddle pinch before turning toward the binary edge.

Summary and Conclusions

We have developed a quick and reliable method for estimating reactive composition profiles in a double-feed reactive

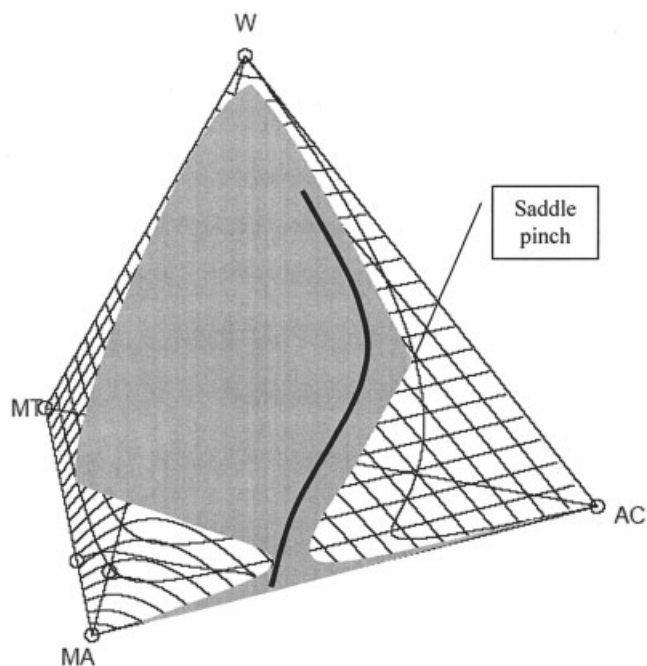


Figure 12. Tray-by-tray-calculated column profile and the feasible region. $r_{\text{ext}} = 2.30$, IRR of the saddle pinch = 2.993, $x_D = [0.001 \ 0.008 \ 0.990 \ 0.001]$, $x_E = [1 \ 0 \ 0 \ 0]$, $x_F = [0 \ 1 \ 0 \ 0]$, $E/D = 1.0$.

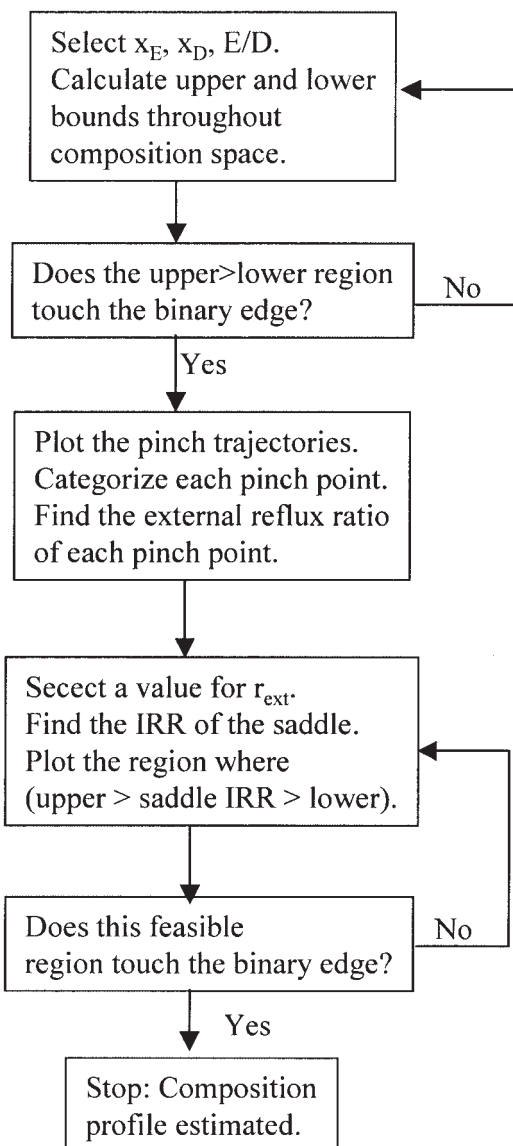


Figure 13. Estimation of feasible reactive composition profiles.

distillation column. Its implementation procedure is summarized in Figure 13. For given entrainer and product compositions, E/D ratio, and phase and reaction equilibrium data, the upper and lower bounds of the internal reflux ratio are calculated throughout composition space. Then, we determine the region where the upper bound is greater than the lower bound. If this region does not extend to the desired binary edge, then a feasible column is not possible for the parameters chosen and a different set of parameters should be selected as shown in Figure 13. Then the continuation method is applied to find pinch trajectories and their dynamic properties. The last step is to select an external reflux ratio for the column and determine the saddle pinch associated with that external reflux ratio. Finally, we draw the feasible region of all liquid compositions where the upper and lower bounds of the internal reflux ratio include the internal reflux ratio of the saddle pinch.

In the proposed scheme of estimating possible composition

profiles for the middle section of reactive and nonreactive extractive distillation columns, only phase and reaction equilibrium calculations with the pinch point analysis are needed to replace rigorous tray-by-tray calculations. From the pinch analysis, the column feasibility and the feasible range of the operating parameters are determined by using the concept of the upper and lower bounds of the internal reflux ratio.

This method can be used in combination with other shortcut design methods, such as the rectification body method^{9,16,18-19} to implement the nonlinearity of column profiles and to determine key design parameters. By combining the concept of critical composition regions⁷, it can also be used to screen suitable entrainers for a particular separation before conducting extensive bench scale separation experiments. Adapting this method to estimate profiles for systems with multiple components and reactions will be the subject of future work in this area.

Acknowledgments

The corresponding author is grateful for the support of Professional Staff Congress City University of New York (PSC-CUNY), and American Chemical Society - Petroleum Research Fund (ACS-PRF, G). The authors are also thankful to Prof. Marquardt at RWTH for his permission to use the code of a shortcut algorithm.

Notation

D = molar flow rate of the distillate stream.
 E = molar flow rate of the extractive (upper feed) stream.
 f_i = mole fraction of chemical component i in the liquid phase of a pinched stage.
 h_D = specific enthalpy of the liquid distillate (exiting the total condenser).
 H_D = specific enthalpy of the vapor distillate (entering the total condenser).
 h_E = specific enthalpy of the extractive (upper feed) stream.
 h_n = specific enthalpy of the liquid leaving stage n .
 H_n = specific enthalpy of the vapor leaving stage n .
 IRR = internal reflux ratio (L_n/D)
 \bar{J} = jacobian matrix of the derivatives of f_i with respect to x_j .
 K_{equil} = reaction equilibrium constant.
 L_n = molar flow rate of the liquid leaving stage n .
 N_{comp} = number of chemical components.
 N_{param} = number of continuation method parameters.
 $normal_i$ = i -th parameter in the vector pointing from the first known pinch point to the second known pinch point in the continuation method scheme.
 r_{ext} = external reflux ratio (L_0/D)
 V_n = molar flow rate of the vapor leaving stage n .
 x_i = value of parameter i of the next pinch point determined by the continuation method
 $x_{D,i}$ = mole fraction of chemical component i in the distillate.
 $x_{E,i}$ = mole fraction of chemical component i in the extractive feed.
 $x_{i,guess}$ = value of parameter i in the initial guess for the next pinch point in the continuation method.
 $x_{n,i}$ = mole fraction of chemical component i in the liquid leaving stage n .

$y_{n,i}$ = mole fraction of chemical component i in the vapor leaving stage n .

Greek Letters

δ_n = cascade difference point at stage N
 $\gamma_{n,i}$ = activity coefficient of component i on stage n
 ν_i = stoichiometric coefficient of component i
 ξ_n = cumulative reaction extent from the top of the column to stage n

Literature Cited

- Agreda VH, Partin LR. Reactive distillation process for the production of methyl acetate. U.S. Patent 4,435,595 (1984).
- Agreda VH, Partin LR, Heise WH. High purity methyl acetate via reactive distillation. *Chem. Eng. Prog.* 1990;86:40-46.
- Knapp JP, Doherty MF. Thermal integration of homogeneous azeotropic distillation sequence. *AIChE J.* 1990;36:969-984.
- Knapp JP, Doherty MF. Minimum entrainer flows for extractive distillation: a bifurcation theoretic approach. *AIChE J.* 1994;40:243-268.
- Wahnschafft OM, Westerberg AW. The product composition regions of azeotropic distillation columns. 2. Separability in two-feed columns and entrainer selection. *Ind. Eng. Chem. Res.* 1993;32:1108-1120.
- Lelkes Z, Lang P, Benadda B, Moszkowicz P. Feasibility of extractive distillation in a batch rectifier. *AIChE J.* 1998;44:810-822.
- Lee JW. Feasibility studies on quaternary reactive distillation systems. *Ind. Eng. Chem. Res.* 2002;41:4632-4642.
- Julka V, Doherty MF. Geometric behavior and minimum flows for nonideal multicomponent distillation. *Chem. Eng. Sci.* 1990;45:1801-1822.
- Bausa J, Watzdorf Rv, Marquardt W. Shortcut methods for nonideal multicomponent distillation: 1. Simple columns. *AIChE J.* 1998;44:2181-2198.
- Reeder C, Remme U, Bausa J, Marquardt W. Design of reactive distillation processes using a new shortcut method for minimum-reflux calculation. *AIChE Annual Meeting*, Miami, November (1998).
- Hauan S, Ciric AR, Lien KM, Westerberg AW. Difference points in extractive and reactive cascades. I - Basic properties and analysis. *Chem. Eng. Sci.* 2000;55:3145-3159.
- Lee JW, Hauan S, Westerberg AW. Feasibility of a reactive distillation column with ternary mixtures. *Ind. Eng. Chem. Res.* 2001;40:2714-2728.
- Song W, Venimadhavan G, Manning JM, Malone MF, Doherty MF. Measurement of residue curve maps and heterogeneous kinetics in methyl acetate synthesis. *Ind. Eng. Chem. Res.* 1998;37:1917-1928.
- Seydel R, Hlavacek V. Role of continuation in engineering analysis. *Chem. Eng. Sci.* 1987;42:1281-1295.
- Seider WD, Brenkel DD, Widagdo S. Nonlinear analysis in process design. *AIChE J.* 1991;37:1-38.
- Brüggemann S, Marquardt W. Shortcut methods for nonideal multicomponent distillation: 3. Extractive distillation columns. *AIChE J.* 2004;50:1129-1149.
- Andersen HW, Laroche L, Morari M. Effect of design on the operation of homogeneous azeotropic distillation. *Comp. Chem. Eng.* 1995;19:105-122.
- Watzdorf Rv, Bausa J, Marquardt W. Shortcut method for non-ideal multicomponent distillation: 2. Complex columns. *AIChE J.* 1999;45:1615-1628.
- Lee JW, Brüggemann S, Marquardt W. Shortcut method for kinetically controlled reactive distillation systems. *AIChE J.* 2003;49:1471-1487.

Manuscript received Dec. 16, 2003, and revision received July 6, 2004.